Serrano-Claumarchirant. José F.; Brotons-Alcázar, I.; Culebras, M.; Sanchis Sánchez, MJ.; Cantarero, A.; Muñoz-Espí, R.; Gomez, C. (2020). Electrochemical Synthesis of an Organic Thermoelectric Power
Generator. ACS Applied Materials & Interfaces. 12(41):46348-46356.
https://doi.org/10.1021/acsami.0c12076

Electrochemical Synthesis of an Organic Thermoelectric Power Generator

José F. Serrano-Claumarchirant,[†] *Isaac Brotons,*[‡] *Mario Culebras,*[§] *Maria J. Sanchis,*[¤] *Andrés Cantarero,*[‡] *Rafael Muñoz-Espí,*[†,*] *Clara M. Gómez,*[†,*]

† Institute of Materials Science (ICMUV), Universitat de València, c/Catedràtic José Beltrán 2, 46980 Paterna, Spain

‡ Institute of Molecular Science (ICMol), Universitat de València, c/Catedràtic José Beltrán 2, 46980 Paterna, Spain

§ Stokes Laboratories, Bernal Institute, University of Limerick, Limerick, Ireland

¤ Department of Applied Thermodynamics, Institute of Electrical Technology (ITE), Universitat Politècnica de València, Valencia, Spain

KEYWORDS: thermoelectric generator, textiles, carbon nanotubes, PEDOT, energy harvesting, layer-by-layer, electrochemical deposition.

ABSTRACT: Energy harvesting through residual heat is considered one of the most promising ways to power wearable devices. In this work, thermoelectric textiles were prepared by coating the fabrics, first with multiple-wall carbon nanotubes (MWCNTs) by using the layer-by-layer technique, and second with poly(3,4-ethylenedioxythiophene) (PEDOT) deposited by

electrochemical polymerization. Sodium deoxycholate and poly(diallyldimethylammonium chloride) were used as stabilizers to prepare the aqueous dispersions of MWCNTs. The electrochemical deposition of PEDOT on the MWCNT-coated fabric was carried out in a three electrodes electrochemical cell. The polymerization of PEDOT on the fabric increased the electrical conductivity ten orders of magnitude (through the plane), establishing an excellent path for the electric transport across the fabrics. In addition, the fibers showed a Seebeck coefficient of 14.3 μV K^{-1}, which is characteristic of highly doped PEDOT. As a proof of concept, several thermoelectric modules were made with different elements based on the coated acrylic and cotton fabrics. The best generator made of 30 thermoelectric elements using acrylic fabrics exhibited an output power of 0.9 μW with a temperature difference of 31 K.

Introduction

The demand for wearable electronic devices has increased enormously in the last years, being biomedical devices, such as blood pressure, temperature, and glucose sensors, one of the main applications. An ideal scenario is the integration of these devices into textiles, which can results in high flexibility, wear resistance, and easy integration in clothes.[1-3] Wearable electronic devices are indeed used in a wide variety of applications, including pressure sensors, [4, 5] photovoltaics,[6, 7] supercapacitors,[8, 9] and wearable power generator devices.[10, 11]. The main problem in all cases is the need for a power supply, typically in the form of batteries and supercapacitors, which have the need to be recharged.[12]

Thermoelectric materials can harvest thermal energy into useful electrical energy. A thermoelectric device converts thermal into electrical energy, and vice versa. The thermoelectric efficiency of a material is given by the dimensionless figure of merit, $ZT = S^2\sigma T/\kappa$, where T is

the absolute temperature; and S, σ, and κ are the Seebeck coefficient, electrical conductivity, and thermal conductivity, respectively.[13]

The total heat dissipation power of an adult human body, by assuming that the body temperature is 37 °C at rest, is approximately 116 W.[14, 15] The theoretical maximum efficiency obtained when a heat engine is operating between two temperatures, the Carnot (η_C) efficiency, is given by the equation

$$\eta_C = \frac{T_{\text{hot}} - T_{\text{cold}}}{T_{\text{cold}}} \times 100 \qquad (1)$$

where T_{hot} is the body temperature and T_{cold} is the ambient temperature. If the ambient temperature varies between 263 and 308 K, the Carnot efficiency will decrease from 17.87% to 0.65%. Therefore, the maximum power available is obtained by assuming a body temperature of 37 °C and an ambient temperature of −10 °C,[16] enabling the production of electric power from the human body with a highly efficient thermoelectric device and supplying energy to wearable devices without the need of recharging.

For the previous reasons, the development of wearable flexible thermoelectric generators has been an active subject of study in recent years. For example, Leonov et al.[17] integrated ceramic-based thermoelectric generators (TEGs) based on Bi_2Te_3 into clothing along with a heatsink reaching a power supply of 100 μW/cm^3 at room temperatures. Other studies were focused on the development of printed flexible thermoelectric devices. Cao et al.[18] used inorganic thermoelectric materials ($Bi_{1.8}Te_{3.2}$ and Sb_2Te_3) mixed with a binding polymer (epichlorohydrin polyglycol-based epoxy) to produce a screen-printable paste reaching a power supply of 2304 nW with ΔT = 20 ºC. However, the vast majority of TEGs made from textiles depicts low flexibility or contain heavy and toxic metals, limiting their practical use.

Looking at this scenario, the selection of materials to make high performing TEG devices is crucial. Due to its high electrical conductivity, flexible nature, environmental stability, and facile synthesis, conducting polymers are good candidates to develop wearable thermoelectric devices, considering that the figure of merit has been improved several orders of magnitude due to effective doping mechanisms.[13, 19-27] However, the main problem of conductive polymers is to show their maximum thermoelectric efficiency in thin films that involves the manufacture of high internal resistance devices, not suitable for energy production.[28] Another problem of conductive polymers is their low adhesion to the fabric substrates, which causes a continuous exfoliation that progressively decreases the conductivity.[29] In this context, the electrochemical synthesis of conductive polymers on fabrics coated with carbon nanotubes (CNTs) could be an alternative to prevent exfoliation, since polymerization occurs on CNTs, which can adhere strongly to the fabric by using compatibilizing agents like polydopamine (PDA), in which the catechol and amine groups ensure strong adhesion.[30] In addition, the electrochemical synthesis is also a good method to control the growth of the film on the fabric substrate.[31] Furthermore, it allows for easily controlling the level of doping with an electrochemical cell. Accordingly, thermoelectric properties can be controlled to achieve a maximum efficiency.[19, 20, 32]

In this study, we develop flexible thermoelectric devices based on multiple-wall carbon nanotubes (MWCNTs) and poly(3,4-ethylenedioxythiophene) (PEDOT). First, MWCNTs are deposited by the layer-by-layer technique to coat the fabric, making it thereby conductive. Then, PEDOT:ClO_4 is polymerized over the fabrics by electrochemical polymerization from the monomer.

Experimental Section

Materials. Poly(diallyldimethylammonium chloride) (PDADMAC) with a molecular weight of 10^5–2×10^5 g mol^{-1} and sodium deoxycholate (DOC) were purchased from Sigma-Aldrich. 3,4-Ethylenedioxythiophene (EDOT), lithium perchlorate, and acetonitrile were purchased from Alfa Aesar. Multiple-wall carbon nanotubes (MWCNTs) were obtained from Bayer Material Science (Leverkusen, Germany, 12–15 nm outer and 4 nm inner wall diameter, length > 1mm, purity 95 wt %). Cotton fabric 400 with a grammage of 100 g m^{-2} was purchased from Testfabrics Inc. (West Pittston PA, USA). Acrylic fabric (made by polyester fibers) with a grammage 140 g m^{-2} and 0.8 mm of thickness was purchased from MW Materials World (Barcelona, Spain). All chemicals were used as received.

Preparation of MWCNT-fabric. Cotton and acrylic fabrics materials were coated with MWCNTs by layer-by-layer deposition to obtain a conducting material. First, fabrics were washed in an ultrasound bath with ethanol for 15 min and dried at 70 ºC overnight. Subsequently, they were dipped in a solution of PDADMAC (0.25 wt%) containing MWCNTs (0.05 wt%) for 2 min. After this process, the fabric was washed with water and drained. Finally, the fabric was dipped in a solution of DOC (0.5 wt %) with MWCNTs (0.5 wt%). The non-attached elements were removed by several washing steps and drained. These two sequential depositions of MWCNTs correspond to one cycle referred to as bilayer (BL). The fabrics were coated with 20 BLs of MWCNTs.

Synthesis of PEDOT on MWCNT-fabrics. The synthesis of PEDOT on MWCNT–fabrics was carried out by electrochemical polymerization applying a current intensity of 6 mA for 4 h. A solution containing EDOT (0.01 M) and $LiClO_4$ (0.1 M) in acetonitrile was prepared. The electrochemical cell was formed by three electrodes: a counter electrode (platinum grid), a

reference electrode (Ag/AgCl), and the MWCNT–fabric, the latter used as the working electrode. The working electrode was assembled as follows to avoid contact between the electrochemical solution and the copper electrodes: the MWCNT–fabric was placed between two pieces of polyethylene terephthalate–indium tin oxide (PET–ITO), one of them connected to a copper tape. Then, PET–ITO sheets with the fabric in between, held with a clamp. The polymerization was carried out in a galvanostatic mode at 6 mA for 4 hours in an IVIUM n-stat apparatus to cover with PEDOT all the dipped part of the fabric. After polymerization, the MWCNT–PEDOT fabric was rinsed several times with acetonitrile and ethanol.

Assembly of thermoelectric modules. The thermoelectric modules were assembled as represented in Figure 1. MWCNT–PEDOT fabrics were cut in small pieces (0.5 cm^2) and attached to a piece of pristine cotton fabric to insulate all the thermoelectric elements in the generator. The bottom and top parts were covered with copper tape (0.5 cm^2) and electrically connected with aluminum wires thermally bounded with tin. The thermoelectric modules were composed of 20 and 30 elements, all connected in series, as shown in Figure 1(b).

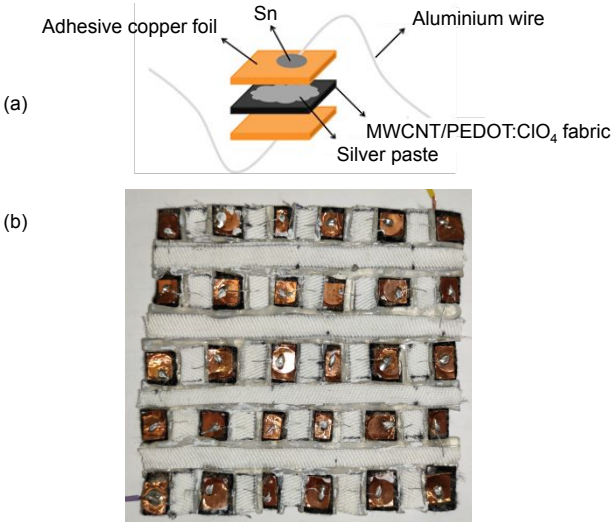

Figure 1. (a) Schematic representation of each element of the thermoelectric module, and (b) photograph of the thermoelectric module.

Characterization. The electrical conductivity was measured in a Novocontrol Broadband dielectric spectrometer (Hundsagen, Germany), integrated by an SR lock-in amplifier with an Alpha dielectric interface to carry out the measurements in the frequency range 10^{-2} to 10^{6} Hz. During all DRS experiments, the samples were placed under a steady flow inert N_2 atmosphere to avoid moisture uptake. Disc-shaped samples of 10 mm of diameter and an approximate thickness of 0.12 mm were mounted in the dielectric cell between two parallel cylindrical gold-plated electrodes. The sample thickness was accurately determined with a micrometer screw. Isothermal measurements (room temperature) were carried out at forty-four frequencies between $5 \cdot 10^{-2}$ and $3 \cdot 10^{6}$ Hz. The experimental uncertainty was less than 5% in all cases.

A home-made device was used for Seebeck effect measurements. The experimental setup consists of two copper blocks, one heated by an electrical resistance and the other cooled by a water flow. The sample is placed between these two blocks. A temperature difference is created across the sample, and the resulting voltage is recorded. The Seebeck coefficient, S, can be determined as the ratio between the electrical potential, ΔV, and the temperature difference, ΔT, that is

$$S = \frac{\Delta V}{\Delta T} \qquad (2)$$

The temperature is controlled by a Lakeshore 340 temperature controller and two Pt100 resistors previously calibrated. An Agilent 34401A multimeter switching system was employed to record the potential. The temperature controller and the multimeter were controlled by using a self-written LabView software. The power supplied was calculated using the expression

$$P = \frac{\Delta V^2}{R_L} \qquad (3)$$

where ΔV is the voltage across the contacts and R_L is the load resistance.

The morphological characterization was carried out by using a Hitachi 4800 S field-emission scanning electron microscope (FE-SEM) at an accelerating voltage of 20 kV and a working distance of 14 mm for palladium-gold coated surfaces.

Raman spectroscopy was performed in a Horiba-MTB Xplora spectrometer with an excitation wavelength of 514 nm. The Raman signal was measured with an open-electrode CCD detector in the 200–2000 cm^{-1} range and the acquisition time was 50 seconds.

The flexibility and stability of the fabrics were carried out in a home-made device. Five twisting cycles of 360º were carried out for each fabric measuring electrical conductivity every 30º, holding the ends of the fabric with two clamps. Bending tests were performed by using a cylinder of 2 cm of diameter and measuring electrical conductivity every 100 bendings.

Results and Discussion

The coating of the fabric surface followed the procedure schematically depicted in Figure 2.[33] MWCNT suspensions were stabilized either with poly(diallyldimethylammonium chloride) (PDADMAC, cationic polyelectrolyte) or with sodium deoxycholate (DOC, anionic surfactant). The assembly of MWCNT bilayers (BLs) is controlled by the electrostatic interaction of these two oppositely charged substances. To optimize the MWCNTs coating process, the cotton and acrylic fabrics were coated with 10, 20, and 30 BLs. The results indicate that the conductivity increases until 20 BLs and reaches a plateau afterward, presumably due to saturation. For the cotton fabric, a plateau is reached after 20 BLs with a conductivity of 2.03×10^{-6} S cm^{-1}, while for the acrylic fabric, the plateau at the same number of BLs reaches a value around 1.5×10^{-7} S cm^{-1}. Since no improvement in the conductivity is observed after 20 BLs, we used this number of layers in the subsequent experiments of polymerization of EDOT on the fabrics.

By using the MWCNT-coated fabric as a working electrode, the effective polymerization of EDOT is achieved by applying a current intensity to the working electrode (MWCNT–fabric).[33] The polymerization mechanism proceeds as follows. Two monomer radicals are initially generated through electrochemical oxidation. Subsequently, the radicals react with each other, forming a dimer and releasing two protons. A new electrochemical oxidation forms an oligomeric radical, which results in the polymer by reacting successively with other oligomeric or monomeric radicals. The electrochemical polymerization of EDOT on the fabrics is also shown in the representation of Figure 2. LbL assembly of MWCNTs by electrostatic interactions was used to coated the fabrics, followed by the electrochemical synthesis of PEDOT:ClO_4. At the beginning of the electrochemical deposition, small polymer nuclei form and serve as centers from which the conductive coat grows.

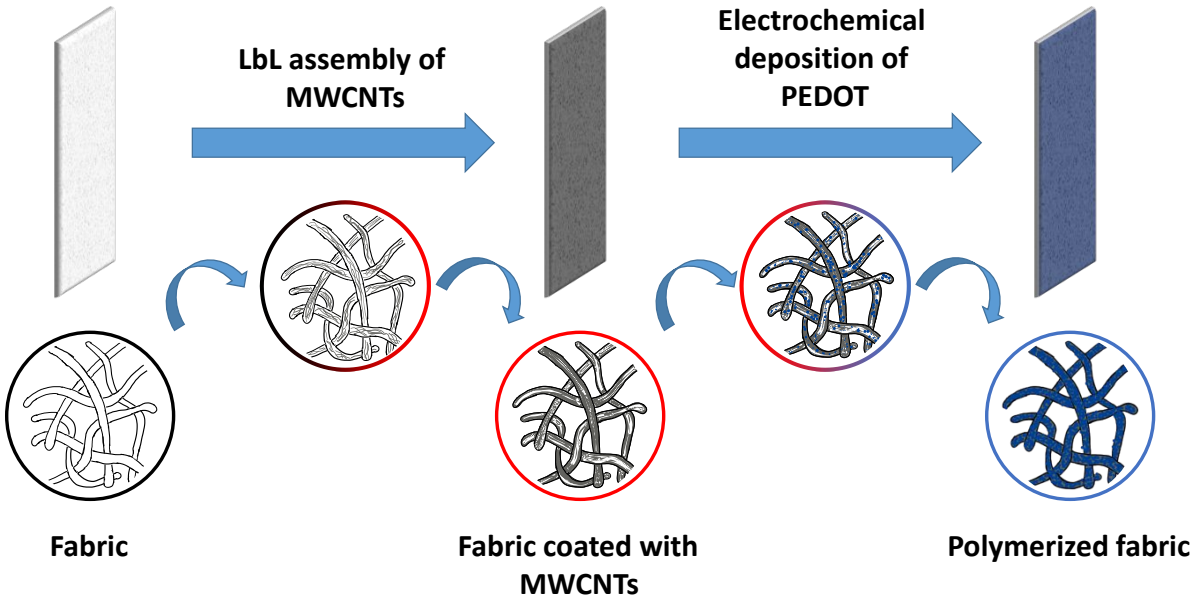

Figure 2. Schematic representation of the preparation of PEDOT by electrochemical deposition on fabric substrates coated with carbon nanotubes through layer-by-layer (LbL).

The effect of the different coatings was analyzed by Raman and infrared spectroscopies spectroscopy, but the latter (spectra shown in Supporting Information, Figure S6) did not offer significant information on the coatings, because the intensities of the MWCNT bands and, especially, PEDOT are weak. However, it can provide information about the nature of the fabrics used. Raman spectra corresponding to cotton fabric substrates, presented in Figure 3, show two regions of signals: 1750–800 cm^{-1} and 610–200 cm^{-1}. The bands in the first region are related to skeletal, symmetric, and asymmetric glycosidic ring breathing (at 1040 and 1128 cm^{-1}), methylene (CH_2) bending, rocking, and wagging (at 1508, 1460, 1356 and 969 cm^{-1}).[34, 35] The second region is given by CCC and COC ring deformation (at 478, 394, 355, and 310 cm^{-1}).[36] Spectra of acrylic substrates present different vibrational modes at 610 and 1274 cm^{-1} related to the C–C aliphatic chain vibration. The peaks at 840 cm^{-1} and 1082 cm^{-1} correspond to the symmetric C–O–C deformation and asymmetric C–O–C deformation, respectively; the peak at 1604 cm^{-1} is related to the aromatic ring chain vibration; and, finally, the peak at 1720 cm^{-1} corresponds to the carbonyl vibration of the ester group. After the coating process of the fabrics with the carbon nanotubes, the intensity of the Raman peaks related to the fabrics decreased and appeared the peaks corresponding to the MWCNTs. The D-band at around 1300 cm^{-1} is ascribed to the presence of disorder in sp^2-hybridized carbon systems. The peak around 1600 cm^{-1} is related to the G-band, which corresponds to sp^2 vibrations of the graphite crystal and is associated with an ordered graphitic structure.[37] Finally, after the electrodeposition of PEDOT, the Raman intensity of the peaks related to the fabrics and the MWCNTs decreased. Therefore, the Raman peaks observed are mainly attributed to the vibrational modes of PEDOT. Peaks at around 420, 560, and 980 cm^{-1} are related to the vibrational modes of oxyethylene ring. The symmetric C–S–C and C–O–C deformation appears at 690 and 1120 cm^{-1}, respectively. The C_α–

C_α (inter-ring) and C_β–C_β stretching modes are located at 1252 and 1363 cm^{-1}, each one. The peak at 1430 cm^{-1} corresponds to the symmetric stretching mode C_α= C_β(–O), and the asymmetric stretching of C=C appears into two Raman peaks at 1490 cm^{-1} (overlapped with the previous peak) and 1530 cm^{-1}.[19] These spectra clearly indicate that all fabrics were well-coated with MWCNTs and PEDOT.

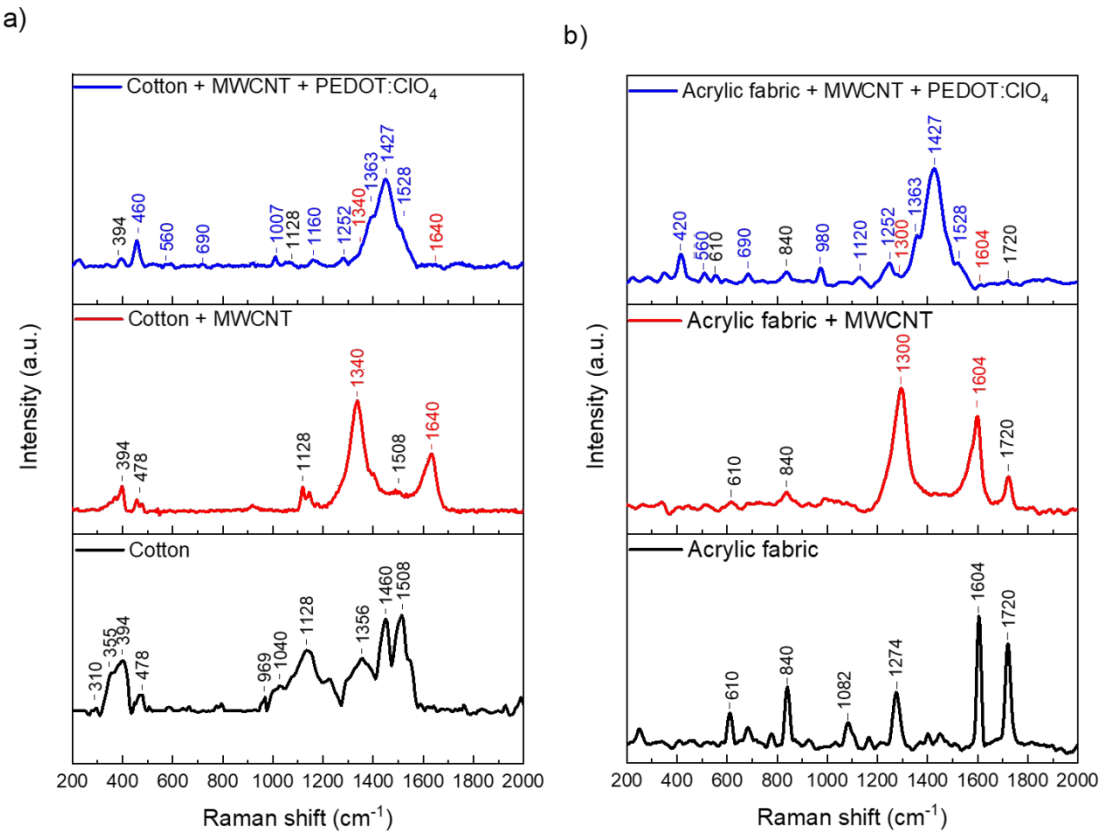

Figure 3. Raman spectra of fabric substrates coated with MWCNT and after PEDOT deposition based on (a) cotton and (b) acrylic fabrics.

The morphology of the PEDOT deposited on the fabrics was studied by scanning electron microscopy (SEM). Micrographs of both fabrics (Figure 4) show that, after deposition, MWCNTs were homogeneously distributed around the fibers, as judged from the lack of

agglomerates. Some bridges observed between fabrics correspond to MWCNTs that electrically connect the fibers. After electrodeposition of PEDOT on the fabrics covered with MWCNT, the polymer is homogeneously distributed around the fabric. SEM images indicate that PEDOT is not only deposited on the superficial layer, but also on most of the internal fibers. PEDOT depicts globular or cauliflower-like morphology, typical from the electrochemical deposition of conducting polymers using chronopotentiometry method.[19, 38, 39]

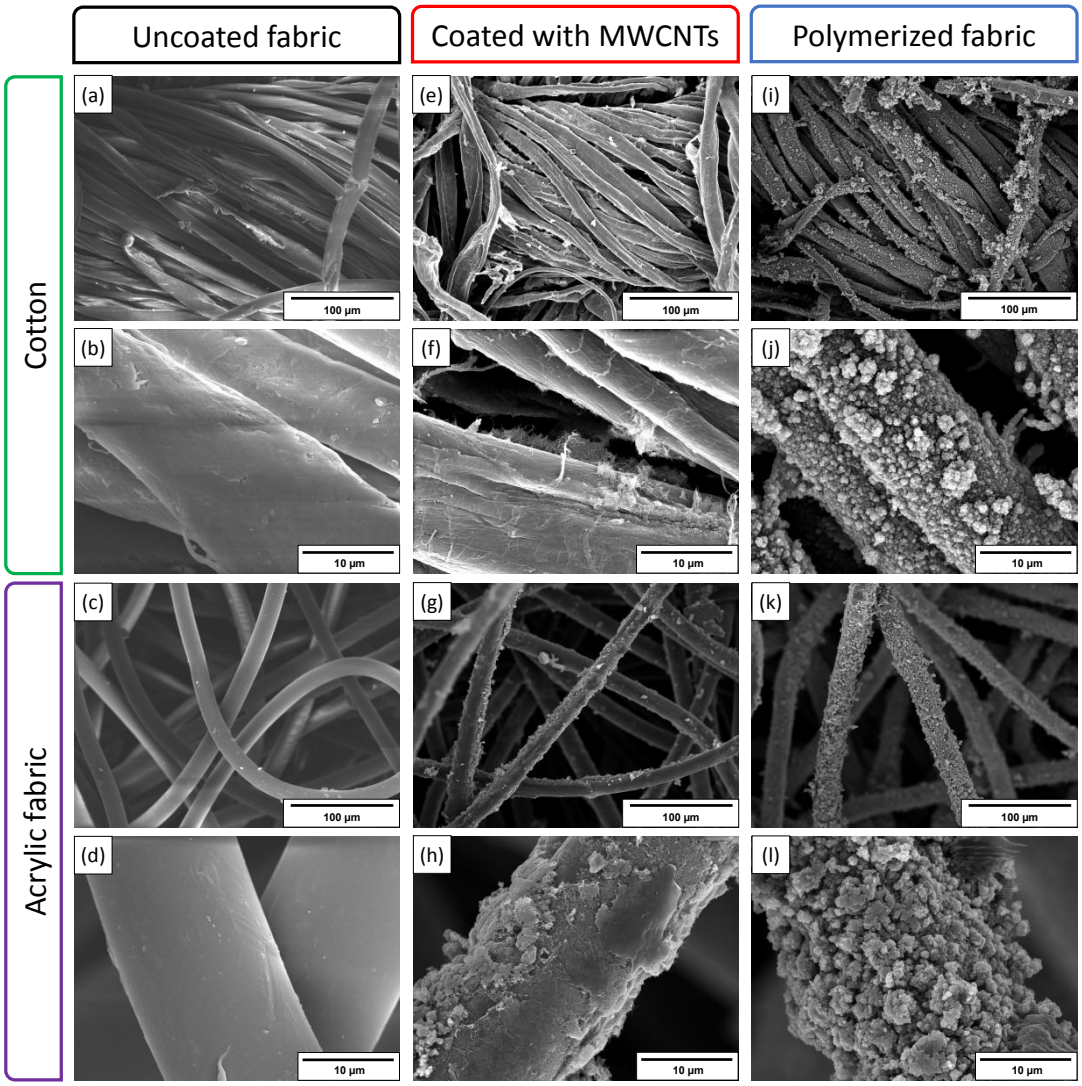

Figure 4. SEM images of uncoated fabrics (a–d), coated with MWCNTs (e–h), and after EDOT polymerization (i–l).

The real component of the complex conductivity $\sigma' = \sigma ac$ (S cm^{-1}) of the fabrics covered with MWCNTs and PEDOT was determined as a function of frequency at room temperature, as showed in Figure 5 for cotton and acrylic fabrics. The electrical conductivity of fabric samples without coating increases as a function of the frequency from 10^{-11} to 10^{-7} S cm^{-1} in the case of cotton, and from 10^{-15} to 10^{-9} S cm^{-1} for acrylic samples, reflecting the dipole polarization contribution to macroscopic conductivity. After the deposition of 20 BLs of MWCNTs onto the fabric samples, the electric conductivity increases, reaching a constant value, independent of the frequency, reflecting that polarization due to charge migration is dominant. Then, PEDOT was deposited by electrosynthesis onto fabrics covered by 20 BLs of MWCNTs, increasing the conductivity by 5 and 6 orders of magnitude for cotton and acrylic fabrics, respectively, compared to fabrics covered with only MWCNTs. The significant increase in the electrical conductivity results from the presence of PEDOT, which acts as an electrical connector between the fibers covered with MWCNTs, making a highly electrically conductive fabric network. Nevertheless, the higher thickness of the acrylic fabric compared to the cotton fabrics can be responsible for the differences observed in the values of the conductivity of both samples. The higher number of interfaces and boundaries in acrylic fabric affect electric transport through the sample, being lower than in the cotton fabric.

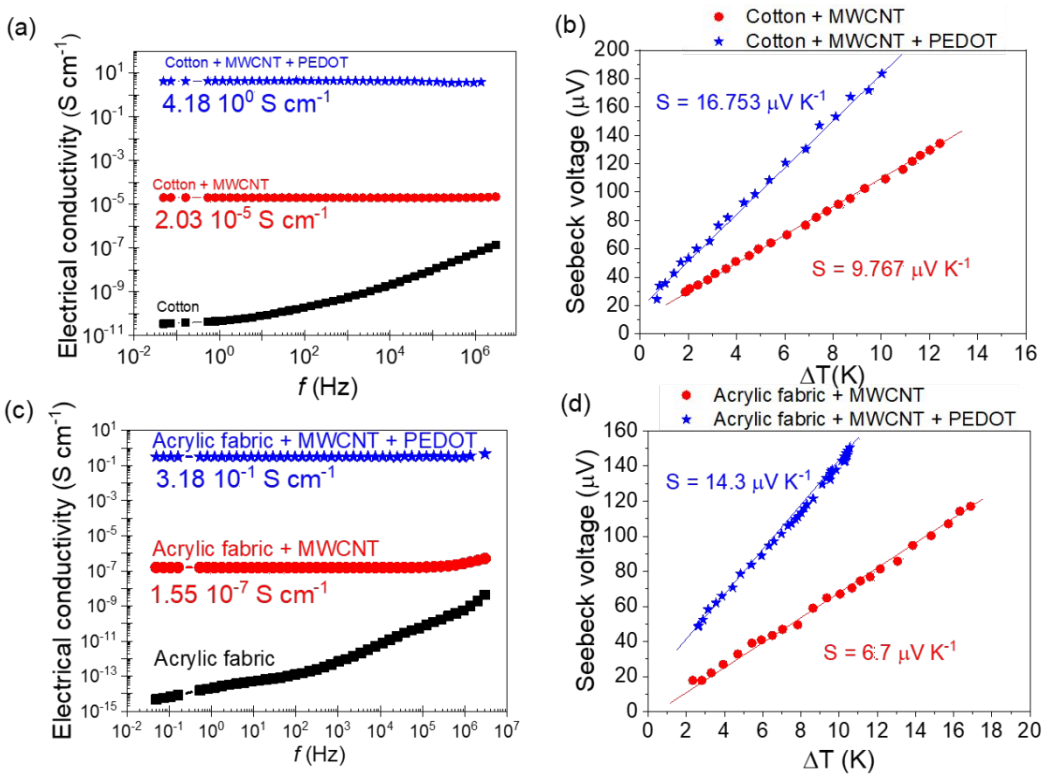

Figure 5. Electrical conductivity at room temperature as a function of the frequency and Seebeck coefficient for cotton fabrics (a, b) and acrylic fabrics (c, d). Uncoated fabrics are represented in black, coated with MWCNTs in red, and after EDOT polymerization in blue.

The Seebeck voltage was measured as a function of the temperature gradient for the fabrics coated with MWCNTs and MWCNTs/PEDOT. It should be noted that the Seebeck coefficient of the uncoated fabrics could not be measured due to its insulating nature. For the case of the fabrics coated with MWCNTs, the Seebeck coefficient was 9.7 μV K^{-1} and 6.7 μV K^{-1} for cotton and acrylic fabrics, respectively. After PEDOT deposition by electrochemical polymerization, the Seebeck coefficient of the fabrics increases until values around 15 μV K^{-1}. These values are very similar to typical ones of PEDOT films and other fabrics coated with

PEDOT,[25, 40-44] evidencing that the whole fabric is coated by PEDOT, which is consistent with the SEM observations (Figure 4).

For the development of fabric-based wearable thermoelectric devices, it is important to evaluate their flexibility and firmness to ensure their stability during everyday use. Therefore, the flexibility and stability of the fabrics coated with MWCNTs and PEDOT were evaluated as a function of the electrical conductivity. For this purpose, five twisting cycles were carried out. The corresponding data, shown in Figure 6, indicate that the electrical conductivity increases as the torsion angle increases, as a result of the improvement of the interconnection between the fibers of the fabrics. This increase is more remarkable in the case of acrylic fabric, which can be correlated with a decrease in the number of boundaries while twisting. The electrical conductivity only decreases as the torsion cycles vary due to the wear that this causes on the fabric. Bending tests, also performed on both fabrics, show that after 3000 bending cycles the electrical conductivity drops by 5% for the case of cotton fabrics and 3% for the acrylics, thus showing high flexibility and stability of the fabrics.

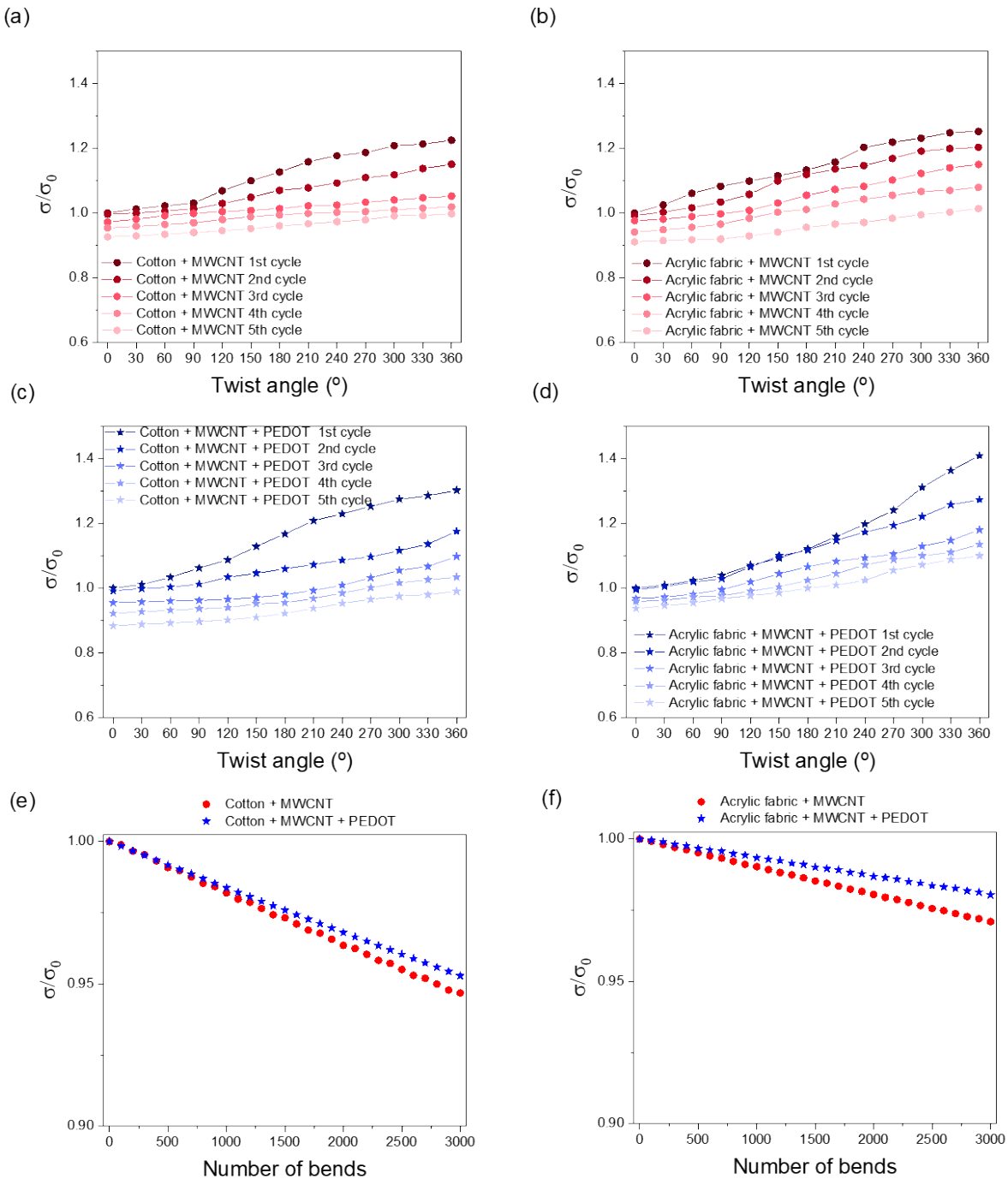

Figure 6. Torsion tests for fabrics coated with MWCNTs (a, b) and after EDOT polymerization (c, d). Bending tests for cotton fabrics (e) and acrylic fabrics (f).

To test the thermoelectric performance of the fabrics, three thermoelectric modules were built as explained in the Experimental Section (Figure 1). The corresponding results are shown in Figure 7. The maximum power of the generator based on cotton fabrics was 47 nW with a temperature difference of 9 K. The other two generators based on acrylic fabrics allowed higher temperature gradients, between 25 and 30 K. This observation can be explained by a greater heat dissipation along with the thermoelectric elements. Thus, the power output increased until 0.3 μW and 0.9 μW for the generator with 20 and 30 elements, respectively, as observed in Figure 7 (b)–(c). In addition, it is worth to highlight the lower internal resistance of the thermoelectric generators (lower than 40 Ω), which indicates that the architecture of the device is adequate for the electron propagation across the thermoelectric elements. These results look very promising when compared to other thermoelectric devices based on fabrics coated with PEDOT:PSS using polyester fabric [16] or using a cleanroom wiper fabric,[43] where they show a TGE with a power output of 12.29 nW at ΔT = 75.2 K and 2 nW at ΔT = 0.6 K, respectively. Other works based on vapor phase polymerization of PEDOT:Cl onto cotton textiles[44] or the deposition of PEDOT:Tos with ionic liquid in different textiles,[29] reached a power output of 4.5 nW at ΔT = 25 K and 62 nW at ΔT = 100 K, respectively. On the other hand, the results obtained are more similar to those obtained by bulk synthesis of PEDOT: Cl (power output 0.375 μW at ΔT = 16.5 K),[45] by alternative doping of carbon nanotube fibers with PEDOT: PSS and oleamine wrapped with acrylic fibers (power output 4.64 μW at ΔT = 44.4 K),[46] or by dipping cotton cellulose fibers with a solution of PEDOT: PSS and ethylene glycol (power output density 2.6 $\mu W \cdot cm^{-2}$ at ΔT = 48.5 K),[47] thus indicating that MWCNTs coated acrylic fabrics and subsequently the electrochemical deposition of PEDOT: ClO_4 are a good alternative for the manufacture of textile-based TEGs.

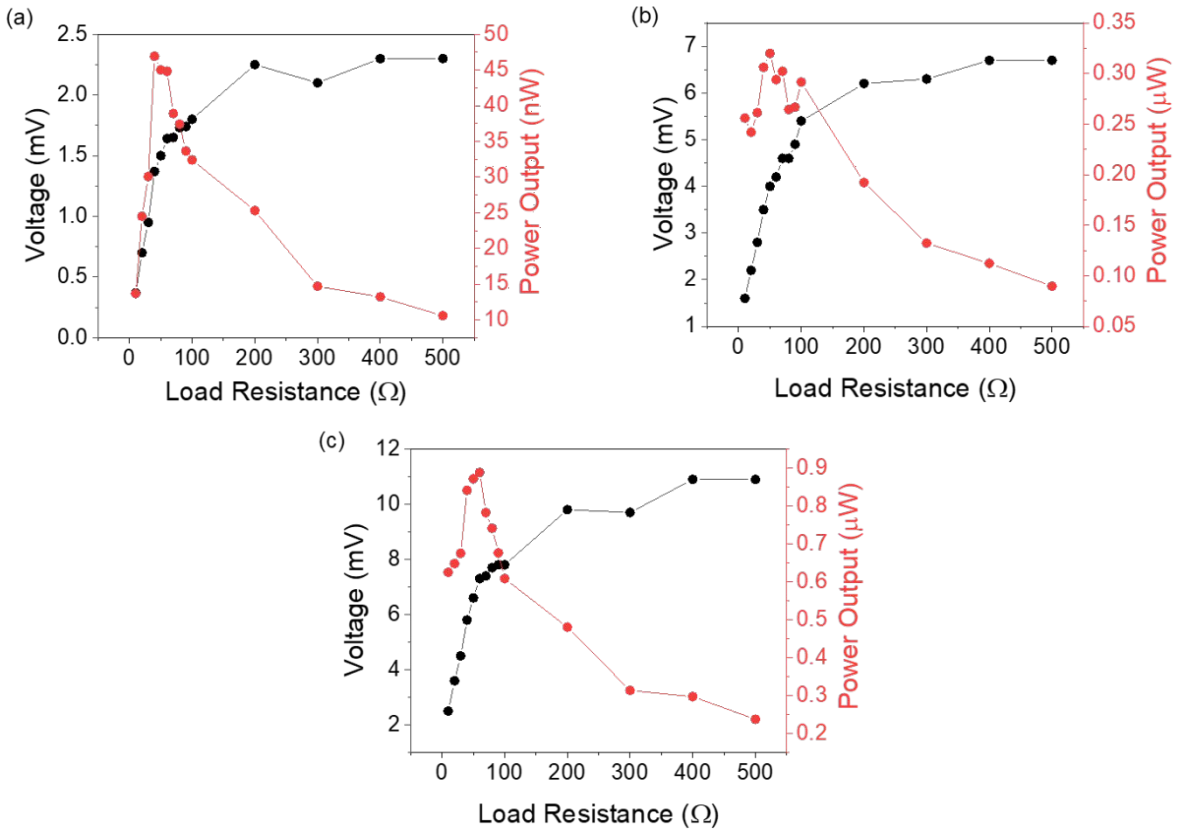

Figure 7. Power generated by the thermoelectric modules composed by (a) 20 elements of cotton/MWCNTs/PEDOT at ΔT= 9 K, (b) 20 elements of acrylic fabric/MWCNTS/PEDOT ΔT= 25 K and (c) 30 elements acrylic fabric/MWCNTS/PEDOT ΔT= 31 K.

Conclusions

Thermoelectric textiles were prepared by coating fabrics with multiple wall carbon nanotubes (MWCNT) through layer-by-layer (LbL) and by electrochemical polymerization of poly(3,4-ethylenedioxythiophene) on its surface. SEM images show that the coating of the acrylic and cotton fabrics with carbon nanotubes is homogeneous and, consequently, the polymerization of the EDOT was also homogeneously carried out on all fibers, increasing the conductivity of the

fabrics by more than ten orders of magnitude. This fact represents a breakthrough in the development of smart textiles and the incorporation of body heat generators since it allows the inclusion of thermoelectric elements into clothes. Moreover, acrylic fabric showed a better performance for fabric-based thermoelectric generators than cotton, because it allows us to establish a higher temperature gradient, and the output power is two orders of magnitude higher.

ASSOCIATED CONTENT

Supporting Information. Additional characterization of fabrics coated with different BLs of MWCNTs and polymerization time.

AUTHOR INFORMATION

Corresponding Authors

*e-mail: clara.gomez@uv.es, rafael.munoz@uv.es

ACKNOWLEDGMENTS

This research was supported by the General Direction of Scientific and Technical Research of the Spanish Government through a grant of the Program Consolider Ingenio (Grant no. CSD2010-0044) and Grant MAT2015-63955-R. J.F.S.-C. acknowledges the financial support by the Spanish Ministry of Education, Culture and Sport through the FPU Training Program. Finally, R.M.-E. thanks the financial support of the Spanish Ministry of Science and Innovation through a Ramón y Cajal grant (Grant no. RYC-2013-13451).

REFERENCES

1. Zhao, Y.; Wang, J.; Li, Z.; Zhang, X.; Tian, M.; Zhang, X.; Liu, X.; Qu, L.; Zhu, S., Washable, Durable and Flame Retardant Conductive Textiles Based on Reduced Graphene Oxide Modification. *Cellulose* **2020**, *27*, 1763-1771.

2. Heo, J. S.; Eom, J.; Kim, Y.-H.; Park, S. K., Recent Progress of Textile-Based Wearable Electronics: A Comprehensive Review of Materials, Devices, and Applications. *Small* **2018,** *14* (3), 1703034.

3. Singha, K.; Kumar, J.; Pandit, P., Recent Advancements in Wearable & Smart Textiles: An Overview. *Mater. Today Proc.* **2019,** *16*, 1518-1523.

4. Lee, J.; Kwon, H.; Seo, J.; Shin, S.; Koo, J. H.; Pang, C.; Son, S.; Kim, J. H.; Jang, Y. H.; Kim, D. E.; Lee, T., Conductive Fiber-Based Ultrasensitive Textile Pressure Sensor for Wearable Electronics. *Adv. Mater.* **2015,** *27* (15), 2433-2439.

5. Doshi, S. M.; Thostenson, E. T., Thin and Flexible Carbon Nanotube-Based Pressure Sensors with Ultrawide Sensing Range. *ACS Sens.* **2018,** *3* (7), 1276-1282.

6. Zhang, N.; Chen, J.; Huang, Y.; Guo, W.; Yang, J.; Du, J.; Fan, X.; Tao, C., A Wearable All-Solid Photovoltaic Textile. *Adv. Mater.* **2016,** *28* (2), 263-269.

7. Ehrmann, A.; Blachowicz, T., Recent Coating Materials for Textile-Based Solar Cells. *AIMS Mater. Sci.* **2019,** *6* (2), 234-251.

8. Dong, L.; Xu, C.; Li, Y.; Huang, Z.-H.; Kang, F.; Yang, Q.-H.; Zhao, X., Flexible Electrodes and Supercapacitors for Wearable Energy Storage: A Review by Category. *J. Mater. Chem. A* **2016,** *4* (13), 4659-4685.

9. Shi, H. H.; Jang, S.; Naguib, H. E., Freestanding Laser-Assisted Reduced Graphene Oxide Microribbon Textile Electrode Fabricated on a Liquid Surface for Supercapacitors and Breath Sensors. *ACS Appl. Mater. Interfaces* **2019,** *11* (30), 27183-27191.

10. Morata, A.; Pacios, M.; Gadea, G.; Flox, C.; Cadavid, D.; Cabot, A.; Tarancón, A., Large-Area and Adaptable Electrospun Silicon-Based Thermoelectric Nanomaterials with High Energy Conversion Efficiencies. *Nat. Commun.* **2018,** *9* (1), 4759.

11. Proto, A.; Penhaker, M.; Conforto, S.; Schmid, M., Nanogenerators for Human Body Energy Harvesting. *Trends Biotechnol* **2017,** *35* (7), 610-624.

12. Pu, X.; Li, L.; Liu, M.; Jiang, C.; Du, C.; Zhao, Z.; Hu, W.; Wang, Z. L., Wearable Self-Charging Power Textile Based on Flexible Yarn Supercapacitors and Fabric Nanogenerators. *Adv. Mater.* **2016,** *28* (1), 98-105.

13. Culebras, M.; Gómez, C. M.; Cantarero, A., Review on Polymers for Thermoelectric Applications. *Materials* **2014,** *7* (9), 6701-6732.

14. Lee, J.; Kim, H. J.; Chen, L.; Choi, S. H.; Mathur, G. N.; Varadan, V. K., Development of Thermoelectric Inks for the Fabrication of Printable Thermoelectric Generators Used in Mobile Wearable Health Monitoring Systems. In *Smart Structures and Materials + Nondestructive Evaluation and Health Monitoring,* Proceedings SPIE, San Diego, California, United States, 2013, 8691R.

15. Du, Y.; Xu, J.; Paul, B.; Eklund, P., Flexible Thermoelectric Materials and Devices. *Appl. Mater. Today* **2018,** *12*, 366-388.

16. Du, Y.; Cai, K.; Chen, S.; Wang, H.; Shen, S. Z.; Donelson, R.; Lin, T., Thermoelectric Fabrics: Toward Power Generating Clothing. *Sci. Rep.* **2015,** *5* (1), 6411.

17. Leonov, V., Thermoelectric Energy Harvesting of Human Body Heat for Wearable Sensors. *IEEE Sens. J.* **2013,** *13* (6), 2284-2291.

18. Cao, Z.; Tudor, M. J.; Torah, R. N.; Beeby, S. P., Screen Printable Flexible BiTe–SbTe-Based Composite Thermoelectric Materials on Textiles for Wearable Applications. *IEEE Trans. Electron Devices* **2016,** *63* (10), 4024-4030.

19. Culebras, M.; Gómez, C. M.; Cantarero, A., Enhanced Thermoelectric Performance of PEDOT with Different Counter-Ions Optimized by Chemical Reduction. *J. Mater. Chem. A* **2014,** *2* (26), 10109-10115.

20. Culebras, M.; Uriol, B.; Gómez, C. M.; Cantarero, A., Controlling the Thermoelectric Properties of Polymers: Application to PEDOT and Polypyrrole. *Phys. Chem. Chem. Phys.* **2015,** *17* (23), 15140-15145.

21. Serrano-Claumarchirant, J. F.; Culebras, M.; Cantarero, A.; Gómez, C. M.; Muñoz-Espí, R., Poly(3,4-Ethylenedioxythiophene) Nanoparticles as Building Blocks for Hybrid Thermoelectric Flexible Films. *Coatings* **2019,** *10* (1), 22.

22. Gómez, C. M.; Culebras, M.; Cantarero, A.; Redondo-Foj, B.; Ortiz-Serna, P.; Carsí, M.; Sanchis, M. J., An Experimental Study of Dynamic Behaviour of Graphite–Polycarbonatediol Polyurethane Composites for Protective Coatings. *Appl. Surf. Sci.* **2013,** *275*, 295-302.

23. Redondo-Foj, B.; Ortiz-Serna, P.; Carsí, M.; Sanchis, M. J.; Culebras, M.; Gómez, C. M.; Cantarero, A., Electrical Conductivity Properties of Expanded Graphite–Polycarbonatediol Polyurethane Composites. *Polym. Int.* **2015,** *64* (2), 284-292.

24. Culebras, M.; Igual-Muñoz, A. M.; Rodríguez-Fernández, C.; Gómez-Gómez, M. I.; Gómez, C.; Cantarero, A., Manufacturing Te/PEDOT Films for Thermoelectric Applications. *ACS Appl. Mater. Interfaces* **2017,** *9* (24), 20826-20832.

25. Culebras, M.; Serrano-Claumarchirant, J. F.; Sanchis, M. J.; Landfester, K.; Cantarero, A.; Gómez, C. M.; Muñoz-Espí, R., Conducting PEDOT Nanoparticles: Controlling Colloidal Stability and Electrical Properties. *J. Phys. Chem. C* **2018,** *122* (33), 19197-19203.

26. Culebras, M.; Choi, K.; Cho, C., Recent Progress in Flexible Organic Thermoelectrics. *Micromachines* **2018,** *9* (12), 638.

27. Serrano-Claumarchirant, J. F.; Culebras, M.; Muñoz-Espí, R.; Cantarero, A.; Gómez, C. M.; Collins, M. N., PEDOT Thin Films with n-Type Thermopower. *ACS Appl. Energy Mater.* **2020,** *3* (1), 861-867.

28. Bubnova, O.; Khan, Z. U.; Malti, A.; Braun, S.; Fahlman, M.; Berggren, M.; Crispin, X., Optimization of the Thermoelectric Figure of Merit in the Conducting Polymer Poly(3,4-ethylenedioxythiophene). *Nat. Mater.* **2011,** *10*, 429-433.

29. Jia, Y.; Shen, L.; Liu, J.; Zhou, W.; Du, Y.; Xu, J.; Liu, C.; Zhang, G.; Zhang, Z.; Jiang, F., An Efficient PEDOT-Coated Textile for Wearable Thermoelectric Generators and Strain Sensors. *J. Mater. Chem. C* **2019,** *7* (12), 3496-3502.

30. Sadi, M. S.; Pan, J.; Xu, A.; Cheng, D.; Cai, G.; Wang, X., Direct Dip-Coating of Carbon Nanotubes onto Polydopamine-Templated Cotton Fabrics for Wearable Applications. *Cellulose* **2019,** *26* (12), 7569-7579.

31. Allison, L.; Hoxie, S.; Andrew, T. L., Towards Seamlessly-Integrated Textile Electronics: Methods to Coat Fabrics and Fibers with Conducting Polymers for Electronic Applications. *Chem. Commun.* **2017,** *53* (53), 7182-7193.

32. Taggart, D. K.; Yang, Y.; Kung, S.-C.; McIntire, T. M.; Penner, R. M., Enhanced Thermoelectric Metrics in Ultra-long Electrodeposited PEDOT Nanowires. *Nano Lett.* **2011,** *11* (1), 125-131.

33. Culebras, M.; Cho, C.; Krecker, M.; Smith, R.; Song, Y.; Gómez, C. M.; Cantarero, A.; Grunlan, J. C., High Thermoelectric Power Factor Organic Thin Films through Combination of Nanotube Multilayer Assembly and Electrochemical Polymerization. *ACS Applied Materials & Interfaces* **2017,** *9* (7), 6306-6313.

34. Edwards, H. G. M.; Farwell, D. W.; Webster, D., FT Raman Microscopy of Untreated Natural Plant Fibres. *Spectrochim. Acta A* **1997,** *53* (13), 2383-2392.

35. Kavkler, K.; Demšar, A., Examination of Cellulose Textile Fibres in Historical Objects by Micro-Raman Spectroscopy. *Spectrochim. Acta A* **2011,** *78* (2), 740-746.

36. Was-Gubala, J.; Machnowski, W., Application of Raman Spectroscopy for Differentiation Among Cotton and Viscose Fibers Dyed with Several Dye Classes. *Spectrosc. Lett.* **2014,** *47* (7), 527-535.

37. Montes-Morán, M. A.; Young, R. J., Raman Spectroscopy Study of HM Carbon Fibres: Effect of Plasma Treatment on the Interfacial Properties of Single Fibre/Epoxy Composites. *Carbon* **2002,** *40* (6), 845-855.

38. Castagnola, V.; Bayon, C.; Descamps, E.; Bergaud, C., Morphology and Conductivity of PEDOT Layers Produced by Different Electrochemical Routes. *Synth. Met.* **2014,** *189*, 7-16.

39. Vlamidis, Y.; Lanzi, M.; Salatelli, E.; Gualandi, I.; Fraboni, B.; Setti, L.; Tonelli, D., Electrodeposition of PEDOT Perchlorate as an Alternative Route to PEDOT:PSS for the Development of Bulk Heterojunction Solar Cells. *J. Solid State Electr.* **2015,** *19* (6), 1685-1693.

40. Seki, Y.; Takahashi, M.; Takashiri, M., Enhanced Thermoelectric Properties of Electropolymerized Poly (3,4-ethylenedioxythiophene) Thin Films by Optimizing Electrolyte Temperature and Thermal Annealing Temperature. *Organ. Electron.* **2018,** *55*, 112-116.

41. Massonnet, N.; Carella, A.; Jaudouin, O.; Rannou, P.; Laval, G.; Celle, C.; Simonato, J.-P., Improvement of the Seebeck Coefficient of PEDOT:PSS by Chemical Reduction Combined with a Novel Method for its Transfer Using Free-Standing Thin Films. *J. Mater. Chem. C* **2014,** *2* (7), 1278-1283.

42. Du, Y.; Tian, T.; Meng, Q.; Dou, Y.; Xu, J.; Shen, S. Z., Thermoelectric Properties of Flexible Composite Fabrics Prepared by a Gas Polymerization Combining Solution Coating Process. *Synth. Met.* **2020,** *260*, 116254.

43. Chen; Lwo, Large-Area Laying of Soft Textile Power Generators for the Realization of Body Heat Harvesting Clothing. *Coatings* **2019,** *9* (12), 831.

44. Allison, L. K.; Andrew, T. L., A Wearable All-Fabric Thermoelectric Generator. *Adv. Mater. Technol.* **2019,** *4* (5), 1800615.

45. Khoso, N. A.; Ahmed, A.; Deb, H.; Tian, S.; Jiao, X.; Gong, X. Y.; Wang, J., Controlled Template-Free In-Situ Polymerization of PEDOT for Enhanced Thermoelectric Performance on Textile Substrate. *Organ. Electron.* **2019,** *75*, 105368.

46. Sun, T.; Zhou, B.; Zheng, Q.; Wang, L.; Jiang, W.; Snyder, G. J., Stretchable Fabric Generates Electric Power from Woven Thermoelectric Fibers. *Nat Commun* **2020,** *11* (1), 572.

47. Kirihara, K.; Wei, Q.; Mukaida, M.; Ishida, T., Thermoelectric Power Generation Using Nonwoven Fabric Module Impregnated with Conducting Polymer PEDOT:PSS. *Synth. Met.* **2017,** *225*, 41-48.

Table of Contents Graphic